Barbara LISIECKA[*], Agata DUDEK[**]

MICROSTRUCTURE AND FRICTION PARAMETERS OF THE SURFACE LAYER OF SINTERED STAINLESS STEELS

MIKROSTRUKTURA I PARAMETRY TARCIA WARSTW WIERZCHNICH SPIEKANYCH STALI NIERDZEWNYCH

Key words:	surface layer alloying, Cr_3C_2 coating, surface roughness, coefficient of friction (COF), sintered stainless steel (SSS), gas tungsten arc welding (GTAW).
Abstract:	Sintered stainless steel (SSS) is manufactured using the powder metallurgy technology (PM). SSSs are characterized by a two–phase structure which can be obtained by mixing different proportions of the main structural components (i.e. austenite and ferrite). Taking into account the improvement of functional properties of SSSs, a number of surface modifications have been proposed. This study proposes a method to improve functional properties by formation of chromium carbide coating and alloying the surface by the gas tungsten arc welding (GTAW) process. The results of light optical microscopy and scanning electron microscopy (SEM/EDX), roughness parameters, hardness, and the coefficient of friction are presented.
Słowa kluczowe:	stopowanie warstwy wierzchniej, powłoka Cr_3C_2, chropowatość powierzchni, współczynnik tarcia, spiekana stal nierdzewna (SSS), spawanie łukowe (GTAW).
Streszczenie:	Spiekana stal nierdzewna produkowana jest przy użyciu technologii metalurgii proszków (PM). Metoda ta opiera się na procesach formowania i spiekania oraz pozwala na wytwarzanie elementów o złożonych kształtach. SSS charakteryzują się dwufazową strukturą, którą można uzyskać poprzez mieszanie w dowolnej proporcji głównych składników strukturalnych (tj. austenit i ferryt). Biorąc pod uwagę poprawę właściwości funkcjonalnych spieków, zaproponowano szereg modyfikacji powierzchni. W niniejszym opracowaniu zaproponowano poprawę tych właściwości poprzez wytworzenie powłoki z węglika chromu i stopowanie powierzchni za pomocą spawalniczej metody łukowej GTAW. Przedstawiono wyniki mikroskopii świetlnej i skaningowej mikroskopii elektronowej (SEM/EDX), parametry chropowatości, twardość oraz współczynnik tarcia. Głównym założeniem tego badania była analiza mikrostruktury i współczynnika tarcia warstw powierzchniowych spieków o różnych proporcjach proszków w wyniku procesu stopowania. Zastosowanie powłok z węglika chromu i stopowanie powierzchni poprawia właściwości tribologiczne spieków (tj. współczynnik tarcia).

INTRODUCTION

The sintered stainless steel has gained more and more attention in a variety of engineering fields. Powder metallurgy (PM) is a technology used for manufacturing of sintered stainless steels (SSSs) **[L. 1**, **2]**. Thanks to the modification of the chemical composition, it is possible to obtain a steel structure with different proportions of the basic components (austenite and ferrite). Taking into account this methodology of steel production, it is possible to produce even small components with complex shapes while maintaining the dimensional precision and

[*] ORCID: 0000-0002-0945-3423. Częstochowa University of Technology, Institute of Material Engineering, Faculty of Production Engineering and Materials Technology, Armii Krajowej 19 Avenue, 42-200 Częstochowa, Poland EU, e-mail: lisiecka.barbara@wip.pcz.pl, (34) 3250627.

[**] ORCID: 0000-0001-9115-028X. Częstochowa University of Technology, Institute of Material Engineering, Faculty of Production Engineering and Materials Technology, Armii Krajowej 19 Avenue, 42-200 Częstochowa, Poland EU, e-mail: dudek.agata@wip.pcz.pl, (34) 3250701.

surface quality **[L. 3, 4]**. The automotive industry is the largest consumer of sintered stainless steel (ca. 73% of all sinters). The uses of sintered materials in the various industries are presented in **Fig. 1 [L. 5–7]**.

Sintered stainless steel is characterized by high mechanical strengths, wear resistance, high toughness, and good corrosion resistance. Unfortunately, the sintered stainless steels are a porous material which can reduce their mechanical properties **[L. 8–11]**. To improve the surface properties of SSSs steel, appropriate coating processes or surface treatments are used. The creation of surface layers is aimed at giving these layers a specific structure as well as modifying the shape and roughness. One such modification is the formation of a carbide-based coating **[L. 12–15]**. Taking into account the best mechanical properties and appropriate adhesion to substrate, the most well–known carbide is chromium carbide (Cr_3C_2). The chromium carbide coatings can be produced using methods like the EB–PDV method, the APS method, and HVOF **[L. 16, 17]**.
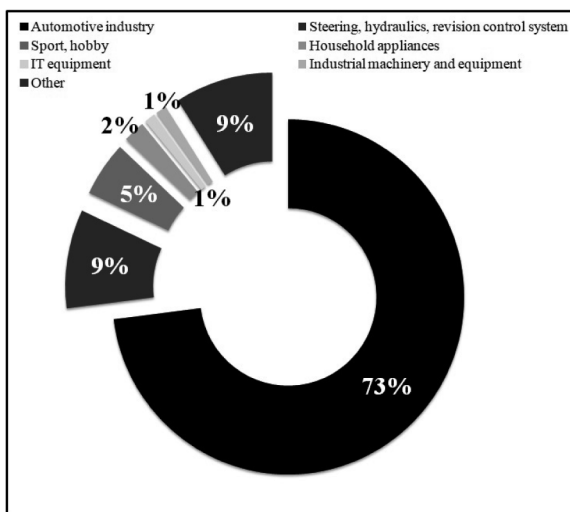

Fig. 1. The use of sintered materials in industries [L. 7]
Rys. 1. Zastosowanie materiałów spiekanych w przemyśle **[L. 7]**

The atmospheric plasma spraying (APS) method is designed for the formation of chromium carbide coatings. The spraying method is based on heating and accelerating the semi-molten coating material (e.g., Cr_3C_2 powder) to the substrate. Such a method of spraying powders results in a dense, adherent, and homogeneous coating. The metallurgical properties of the substrate do not change after coating, because the substrate is not regularly heated up to 150℃. The obtained coatings can be controlled for their properties (e.g., porosity, roughness, and hardness) **[L. 18–23]**.

The laser technologies are the most widespread methods used in surface alloying treatment. In addition to high precision and the ease of automation, these technologies are very expensive processes **[L. 24, 25]**. Therefore, the gas tungsten arc (GTAW method) welding process is increasingly used for the modification of the surface layer of SSSs, which they are showing porosity. Using the GTAW method, it is possible to modify the surface in terms of hardness and the coefficient of friction **[L. 26–29]**.

The authors of the present study propose and emphasize the improved functional properties of sintered stainless steels. In the literature, it is in vain to search for this particular surface modification of sintered stainless steels by applying Cr_3C_2–NiAl coating and alloying with the GTAW method. Numerous research studies undertaken by the authors restated that the use of Cr_3C_2–NiAl coating and GTAW surface alloying methods are promising and inexpensive methods to improve the discussed steel properties.

The purpose of research was to determine the impact of the process of sintering the surface layer of SSSs with different proportions of powders as a result of the alloying process on the structure and the coefficient of friction, which is a new issue in the light of the available literature. The application of the chromium carbide coatings and alloying the surface improve the tribological properties of SSSs (i.e. the coefficient of friction).

MATERIAL AND METHODS

The specimens of sintered stainless steel were made of water–atomized powders of AISI 316L and AISI 409L steels manufactured by Höganäs (Sweden). **Table 1** presents the chemical composition of the steel powders. Both powders selected have a nominal particle size of 150 μm.

Table 1. Chemical composition of steel powders (%wt.)
Tabela 1. Skład chemiczny proszków stalowych (% mas.)

Powder grade	Cr	Ni	Mo	Si	Mn	C	S	Fe
AISI 316L	16.80	12.00	2.00	0.90	0.10	0.022	0.005	Balance
AISI 409L	11.86	0.14	0.02	0.82	0.14	0.020	0.010	Balance

In the examinations, powders mixed at different proportions of austenitic and ferritic steel powders were used to obtain the different series of the samples (see **Table 2**). The powders were compacted uniaxially with the addition of 1% Acrawax C lubricant at 720 MPa. The moulded pieces were sintered at the temperature of 1250°C for 30 minutes and then cooled down with a cooling rate of 0.5°C/s. The whole process was done in reducing atmosphere using 100% hydrogen in order to significantly limit oxidation of the batch and protect from the reduction of the chromium content.

Table 2.   Percentage contribution of individual powders
Tabela 2.   Procentowy udział poszczególnych proszków

Samples number	Powder grade	
	AISI 316L [%wt.]	AISI 409L [%wt.]
U1	80	20
U2	50	50
U3	20	80

The next stage of examination was the creation of a layer from chromium carbide by means of plasma spraying (APS method). The chromium carbide is mechanically mixed with nickel and aluminium (90% wt. Cr_3C_2 and 10% wt. NiAl) and the coating is made at high temperatures. Process parameters are presented in **Table 3**. The resulting coating had a thickness of around 60 μm.

Table 3.   APS method parameters
Tabela 3.   Parametry procesu natryskiwania plazmowego

Working parameters		Ranges
Voltage (U_r)		60 [V]
Current intensity (I_r)		450–500 [A]
Distance of the plasmatron from the surface		80 [mm]
Gas flow rate	Argon	45 [l/min]
	Hydrogen	17 [l/min]

The surface layers of the alloying treatment of the coated SSS were made by means of GTAW technology (gas tungsten arc welding). The process was carried out with a constant surface scanning rate of 340 mm/min and a changing welding current intensity with its values ranging from 50 to 70A. The shielding gas was argon, with the flow set at ~ 14 l/min. **Table 4** presents the parameters used in the alloying process.

Table 4.   Parameters of arc alloying of SSS
Tabela 4.   Parametry obróbki stopowania stali spiekanych nierdzewnych

Samples number	Current intensity I [A]	Arc voltage U [V]	Total arc power q_c [W]	Arc linear energy E [kJ/m]
1	50	11.0	550	97.09
	60	11.5	690	121.81
	70	12.0	840	148.29
2	50	11.5	575	101.51
	60	12.2	732	129.23
	70	11.5	805	142.12
3	50	14.5	725	127.99
	60	11.5	690	121.81
	70	12.0	840	148.29

The macroscopic evaluation of SSSs after the alloying process was performed using a stereo microscope Olympus SZ61. The analysis of the microstructure was carried out using an Olympus GX41 light optical microscope and scanning electron microscope Jeol JSM–6610LV. The Vickers methodology (with the load of 980.7 mN) was employed to measure microhardness of sintered stainless steels, coating, and alloying surface layers.

The Hommel T1000 contact profilometer was used to determine parameters that characterized surface topography (Ra, Rz, and Rmax) for each sample. The measurements were repeated three times in contact with the surface examined through the coupling of the stylus with a differential measurement system.

In order to determine the coefficient of friction for SSSs, the scratch resistance test (Revetest XPress Plus using Rockwell indented tip) was performed. The following parameters were maintained during the test: permanent load of 10 N, scratch length 10 mm, and scratch rate 5 mm/min.

RESULTS AND DISCUSSION

Figure 2 presents photographs of grains of Cr_3C_2–NiAl powder and EDX–analysis of the chemical composition determined by by using the scanning electron microscope.

The chromium carbide coating obtained using plasma spraying on the sintered steel surface had a thickness of ca. 60 μm. **Figure 3** presents the microstructure of the coating surface (before alloying process) determined using a stereo microscope (2a) and the scanning electron microscope (2b).
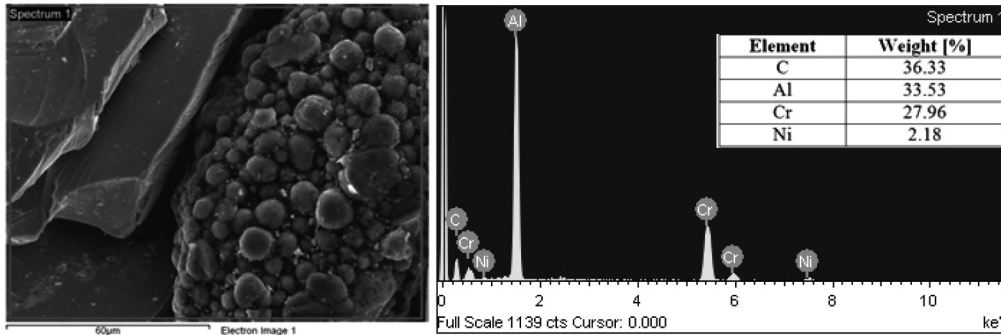

Fig. 2. **Morphology and EDX–analysis of chemical composition of the Cr_3C_2–NiAl powder used to produce the coating**
Rys. 2. Morfologia i analiza składu chemicznego proszku Cr_3C_2–NiAl użytego do wytworzenia powłoki

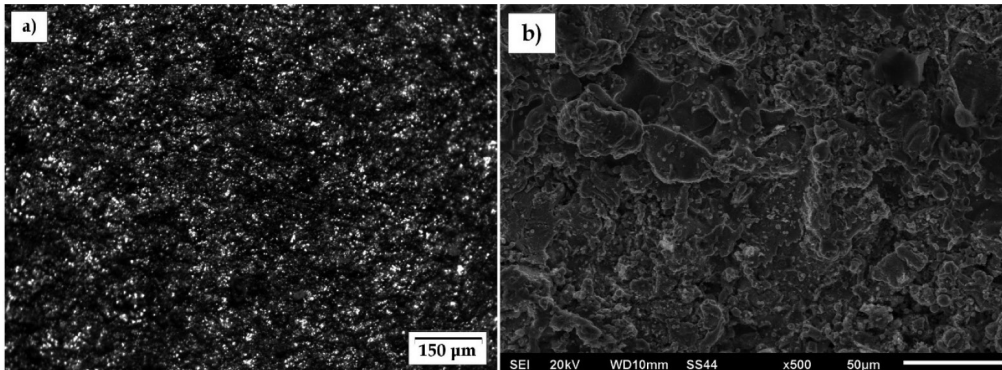**Fig. 3.** **Microstructure of the coating surface on SSS after APS process**
Rys. 3. Mikrostruktura powłoki na powierzchni spieków nierdzewnych po procesie APS

Figure 4 presents the cross–section of the coating microstructure determined using the scanning electron microscope.

The coating obtained in the examinations show elements of structure typical of this method of deposition (porosity, layers, heterogeneity). These coatings exhibit a typical porous lamellar structure with cracks and non–melted particles. The effect of alloying on surface quality of SSS was evaluated by macroscopic examinations. The main criteria that were taken into account during this evaluation were the continuity of the band, and the comparable width and relatively smooth surface without craters. These requirements were met by the bands alloyed using the GTAW method with a current intensity of 60 A. **Figure 5** presents the morphology of the surface after the alloying process at a current intensity of 50 A determined using a stereo microscope.
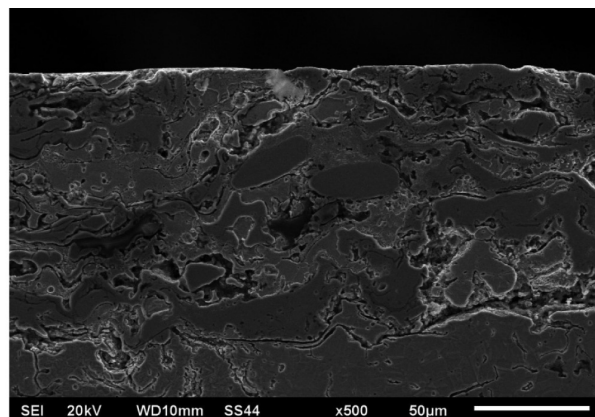

Fig. 4. **Microstructure of the cross–section of coating after APS method**
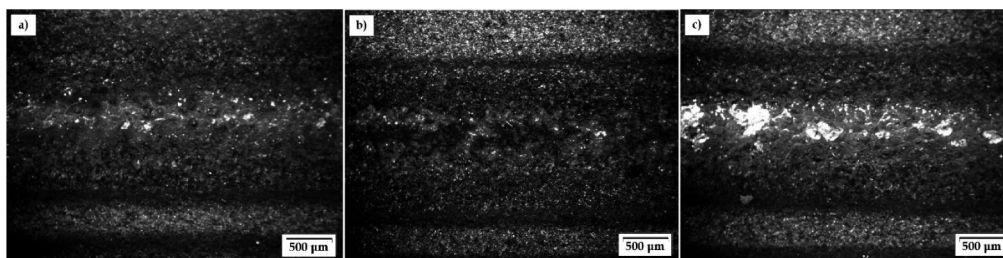Rys. 4. Mikrostruktura przekroju poprzecznego powłoki po procesie APS

Fig. 5.　Morphology of the surface of SSSs after alloying 50 A for samples: a) U1, b) U2, c) U3
Rys. 5.　Morfologia powierzchni spieków nierdzewnych po stopowaniu 50 A dla próbek: a) U1; b) U2; c) U3

The microstructures obtained for SSS after surface alloying treatment were observed using the metallographic sections, which were etched with aqua regia. **Figure 6** presents the microstructure of the surface after alloying at all applied current intensities used by the GTAW method obtained for sample U2 determined by the light optical microscope.
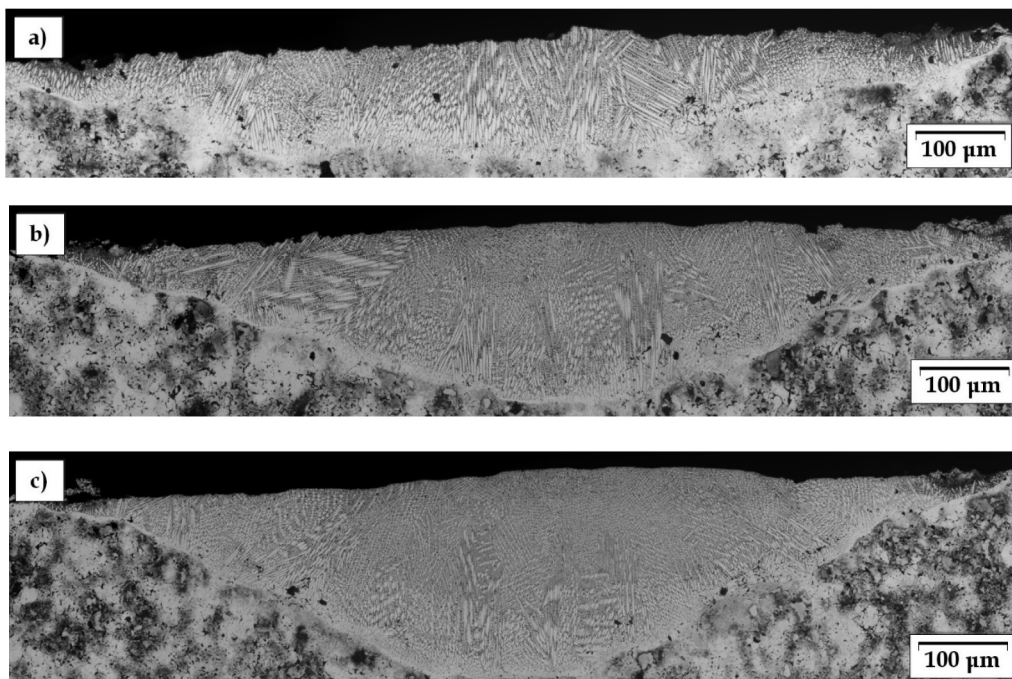

Fig. 6.　Microstructure of the entire alloyed zone for sample U2 after alloying: a) 50 A, b) 60 A, c) 70 A
Rys. 6.　Mikrostruktura strefy stopowanej dla próbki U2 po stopowaniu: a) 50 A; b) 60 A; c) 70 A

Conducted microstructural examinations showed a homogeneous cellular–dendritic structure in the surface layers after alloying treatment. The formation of the primary structure with the columnar crystals oriented in the direction of heat transfer was caused by the fast heat transfer and high gradient of temperature. The transient zone was the location of the epitaxial character of nucleation and the growth of primary structure crystals. In addition, it was observed that none of the sinters samples had a two-phase microstructure typical of conventional stainless steel. The presence of austenite, ferrite, and a phase with martensite morphology was found. A few defects located at the boundary of the alloying zone and the heat affected zone, which are a result of the crystallization process and the GTAW method, were disclosed.

Taking into account microstructure analysis of surface layers, positive examinations results for the bands after alloying at current intensity of 60 A were obtained.

Figure 7 presents the microstructure of the surface after the alloying process for SSS determined using the

scanning electron microscope. Results confirm that the formation of columnar crystals are oriented according to the direction of heat transfer (i.e. perpendicular to the specimens' surface).
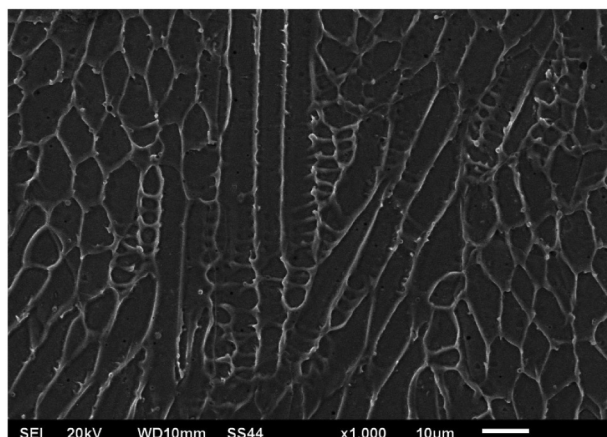

Fig. 7. Microstructure of the surface of sample U1 after alloying at current intensity 60 A – central part of the alloyed zone

Rys. 7. Mikrostruktura powierzchni próbki U1 po stopowaniu 60 A – centralna część strefy stopowanej

As already mentioned, the microstructure analysis has shown that the best results were obtained for samples alloying at a constant intensity of 60 A. Based

on **Figs. 5, 6,** and **7**, and taking into account the quality of the alloying, it can be considered that the best current of intensity of alloying is 60 A. This is conditioned by obtaining the most homogeneous cellular–dendritic structure for this current intensity (60 A) during the alloying of all samples. The analysis of the chemical composition of the surface layers in sintered stainless steels after alloying at a current intensity of 60 A using by the GTAW method was used for comparison and is presented in **Table 5**. The information obtained in the study allowed a comparison of the areas obtained for SSSs after surface treatment, to determine of the migration of alloying elements during the crystallization process and to determine of the degree of homogeneity of the chemical composition in surface layers.

Analysis of the change of the content of the elements revealed the migration of Cr and Ni during sintering caused by the diffusion process. The effect of diffusion was the formation of mutual diffusion areas between the ferritic and austenitic phases. Chromium diffuses to ferrite, while nickel diffuses to austenite, which leads to different phase transformations. Ferrite in its primary structure forms between austenitic cells; therefore, studies have shown that the cores are enriched in Ni, with intercellular areas rich in Cr. The differences in the content of the alloy elements (Cr and Ni) were observed for all the sintered stainless steels, which are related to the migration of elements during solidification.

Table 5. EDX – analysis of chemical composition of the SSSs after alloying at current intensity of 60 A

Tabela 5. Analiza składu chemicznego spiekanych stali nierdzewnych po stopowaniu 60 A

SSSs	Element	Weight [%]		
		Alloying zone	Heat affected zone	Native material
U1	Cr	26.44	21.24	15.39
	Fe	51.37	59.29	71.40
	Ni	17.82	15.30	7.66
	Al	0.14	0.09	–
U2	Cr	17.62	16.12	13.50
	Fe	66.91	67.02	73.08
	Ni	9.66	8.82	6.90
	Al	0.22	–	–
U3	Cr	15.19	14.89	12.32
	Fe	74.97	76.52	74.39
	Ni	7.53	6.73	4.58
	Al	0.09	–	–

The selection of an appropriate coating as well as the parameters of alloying the surface layer that will improve the functional properties of sintered stainless steel is extremely important as well as difficult. As is known, the alloying depends on the shrinkage effect, which can lead to the deformation of the material surface and the cracking of the material. Therefore, it is necessary to choose coatings and alloying parameters to

make the thickening of the material in a small volume. The appropriate selections of coatings and surface treatment have an impact on the reduction of roughness and elimination of porosity.

The profilometric examinations and results of roughness parameters were used for analysis of the geometric structure of the Cr_3C_2 coating and the surface of the SSSs after alloying. The macroscopic analysis

showed that the bands alloyed at a current intensity of 60 A were characterized by an equal width in the arc effected zone and the desired smoothness of the surface. These observations were reflected by the results of roughness tests. **Figure 8** presents the values of obtained profilometric investigations for the surface of SSSs in comparison to the Cr_3C_2 coating. The following parameters were selected for analysis:

– Ra (arithmetic mean roughness deviation from the mean line),
– Rz (maximum height of the profile), and
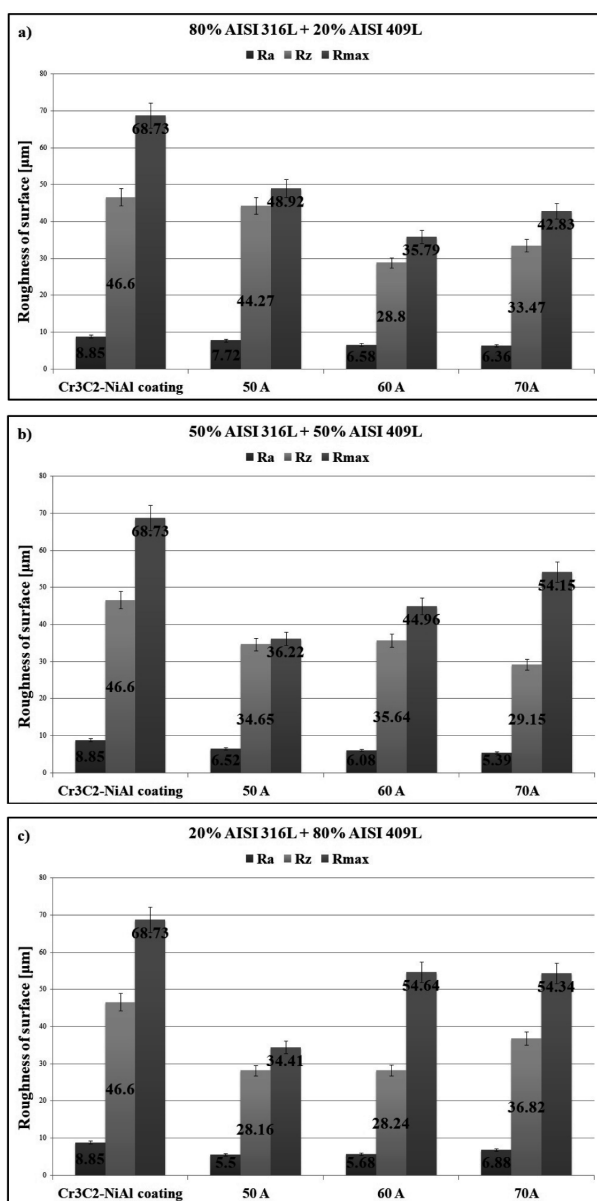– Rmax (maximum distance between a profile peak and the lowest valley).

Fig. 8. Roughness of the surface of SSSs after alloying in compare to Cr3C2 coating for samples: a) U1, b) U2, c) U3

Rys. 8. Chropowatość powierzchni spieków po stopowaniu w porównaniu z powłoką Cr3C2 dla próbek: a) U1, b) U2, c) U3

The surface of the sinters after the creation of the layer from chromium carbide by means of plasma spraying was characterized by a roughness of Ra = 8.85 μm. In the GTAW method, the roughness is reduced, which is related to the amount of energy that was finally delivered to the surface of the alloying metal (arc linear energy). Furthermore, the continuous operation mode of the device guaranteed equal distribution of liquid metal in the alloyed band. The application of this method resulted in an insignificant reduction in surface roughness, which is demonstrated by lower values of, e.g., Ra, Rz and Rmax. The lower values of the Ra parameter were observed in all the alloyed zones compared to the surface of the coating. The highest values of the Ra parameter were obtained for sinters where the participation of the austenitic phase was the highest. In the case of U1 and U2 sinters, the greatest surface smoothing was recorded after alloying at a current intensity of 70 A. This is related to the thermal conductivity which is lower for austenitic and duplex steels (about 15 W/mK) and higher for ferritic and martensitic steels (25–30 W/mK). The surface roughness results confirmed that the best results were obtained for sintered stainless steel after alloying at a current intensity of 60 A. **Figure 9** presents the diagram of profilograph for SSSs after alloying at current intensity of 50 A.

In order to evaluate mechanical properties, hardness measurements were made by the Vickers method. The results present the mean of three measurements in the alloying zone, the heat affected zone, and the native material obtained during and after alloying at the current intensity of 60 A (see **Table 6**). The use of a Cr_3C_2–NiAl coating and the GTAW method led to the homogenization of the microstructure, which was evident in microstructural investigations and confirmed by hardness tests.

The preparation of Cr_3C_2–NiAl coating on sintered stainless steels led to an almost double increase in hardness and consequently to the improvement of the mechanical properties of SSSs. As is well known, the contribution of individual phases and the addition of Cr_3C_2–NiAl powder to the surface layers have direct effects on the mechanical properties of the whole sinter **[L. 30, 31]**. In addition, the use of the GTAW method has led to even greater improvement in properties as reflected by higher hardness values in the alloying zone. The obtained values show improvement in strength properties for all sinters after surface alloying treatment (**Fig. 10**).

Scratch tests under constant load were made to evaluate the coefficient of friction and friction wear resistance. The data obtained as a result of the Scratch Tests are presented in the form of a chart with coefficient of friction and frictional force. **Figure 11** presents an example diagram of normal load and friction for samples U2 after alloying at a current intensity of 60 A obtained by the Scratch Test.
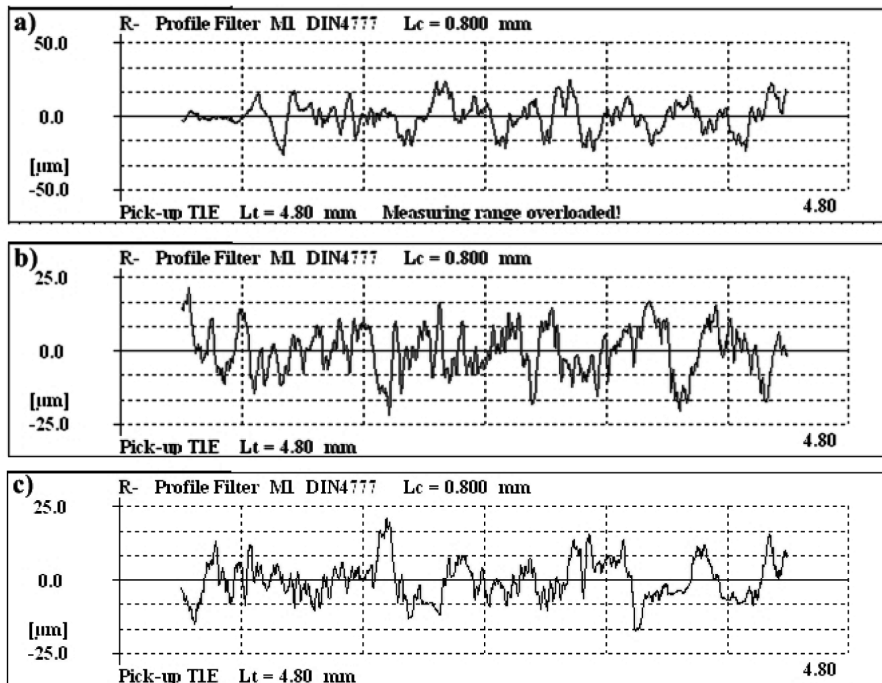
Fig. 9. Diagram of profilograph for SSSs after alloying 50 A for samples: a) U1, b) U2, c) U3
Rys. 9. Schemat profilografu po stopowaniu 50 A dla próbek: a) U1; b) U2; c) U3

Table 6. Hardness of SSSs
Tabela 6. Twardość spiekanych stali nierdzewnych

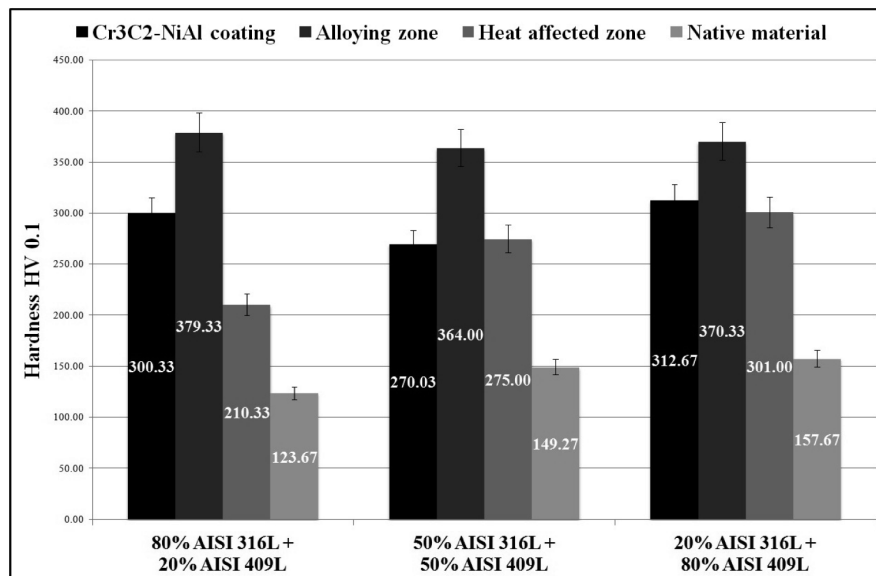| SSSs	Hardness [HV 0.1]			
	Cr$_3$C$_2$–NiAl coating	Alloying zone	Heat affected zone	Native material
U1	300.33 ± 16.34	379.33 ± 8.99	210.33 ± 8.18	123.67 ± 11.81
U2	270.03 ± 7.33	364.00 ± 4.32	275.00 ± 23.87	149.27 ± 8.00
U3	312.67 ± 11.67	370.33 ± 16.82	301.00 ± 47.67	157.67 ± 14.52

Fig. 10. Hardness of SSSs
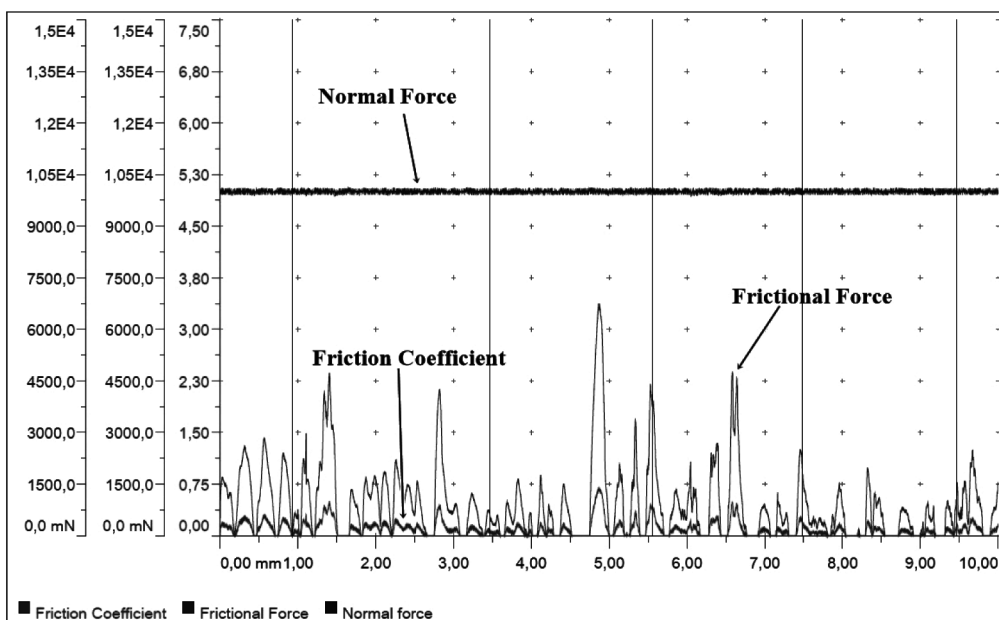Rys. 10. Twardość spiekanych stali nierdzewnych

Fig. 11. Diagram of normal load and friction for sample U2
Rys. 11. Wykres obciążenia normalnego i tarcia dla próbki U2

The comparison of scratch test results was possible for various specimens, since the same indenter rate, force, and type of indenter were used. **Figure 12** presents the coefficients of friction for SSSs after alloying.

The factors, such as chemical composition, proportion of individual powders, sintering conditions, hardness, and porosity, have an influence on the resistance to friction wear of SSSs. It is assumed that the lower the coefficient of friction, the greater is the resistance to abrasive wear. Furthermore, increasing the percentage content of ferrite improves tribological properties. As a result of the tests, it was shown that samples U2 has the lowest coefficient of friction in all possible modifications compared to other sinters. The modification of the coefficient of friction proposed in this article contributes to the improvement of tribological properties of sinters.
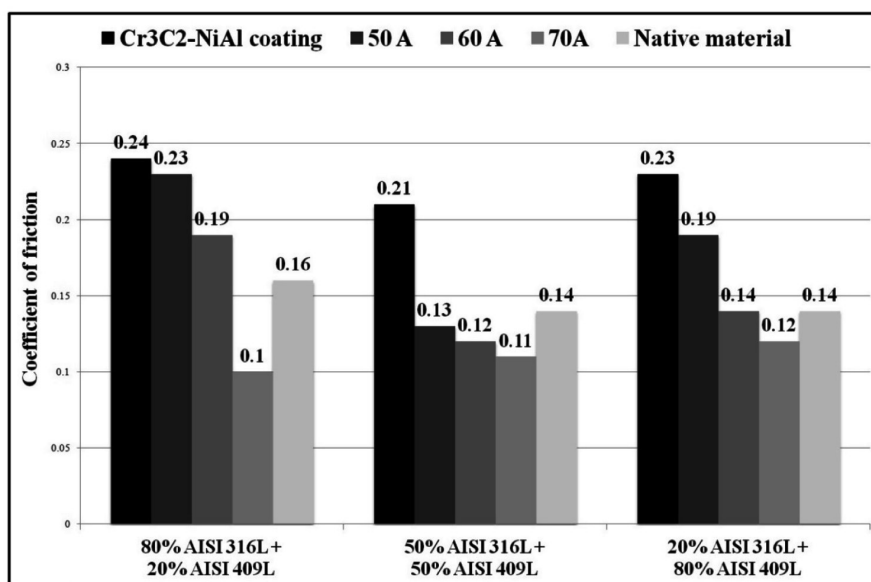

Fig. 12. Coefficient of friction for the SSSs: a) U1, b) U2, c) U3
Rys. 12. Współczynnik tarcia dla spiekanych stali nierdzewnych po stopowaniu: a) U1; b) U2; c) U3

CONCLUSIONS

Cognitive conclusion:

In this article, characteristic of Cr_3C_2–NiAl coating and surface layers on SSSs after alloying by GTAW method are presented. The method proposed by the authors is a promising and inexpensive method to improve the functional properties of sintered stainless steels. Sintered materials were prepared from mixtures of stainless steel series 316 and series 409 powders. The chromium carbide (Cr_3C_2–NiAl) was applied to prepare the coating by the APS method. The use of this powder causes that the obtained coating has excellent strength, hardness, and wear resistance.

Utilitarian conclusion:

The study shows that the alloying method used by the authors is a promising proposal for the hardening of the surface layers of SSSs that show porosity. The gas tungsten arc welding (GTAW) method represents an alternative solution compared to the laser technique. It was observed that the increase in current intensity causes a decrease in the coefficient of friction and an increase in hardness, which consequently leads to the increased wear resistance. The wear resistance also depends on the percentage content of the individual powder (austenite or ferrite) in the particular sinter. The best results were obtained for sintered stainless steels after alloying at current intensity of 60 A. The alloying of the samples at this current intensity affected the achievement of a homogeneous cell–dendritic structure. The chemical composition, the proportion of individual powders, sintering conditions, the suitable coating, and the current intensity, affects the tribological properties of SSSs.

Development conclusion:

In further stages of research, the authors plan to carry out corrosion tests and determine the impact of the alloying process for the corrosion resistance of produced materials.

REFERENCES

1. Martín F., García, C., Blanco Y., Rodriguez-Mendez M.L.: Influence of sinter-cooling rate on the mechanical properties of powder metallurgy austenitic, ferritic, and duplex stainless steels sintered in vacuum. Materials Science & Engineering A, 2015, vol. 642, pp. 360–365.
2. Peruzzo M., Beux T.D., Ordonez M.F.C., Souza R.M., Farias M.C.M.: High-temperature oxidation of sintered austenitic stainless steel containing boron or yttria. Corrosion Science, 2017, vol. 129, pp. 26–37.
3. Shojaati, M., Beidokhti, B.: Characterization of AISI 304/AISI 409 stainless steel joints using different filler materials. Construction and Building Materials, 2017, vol. 147, pp. 608–615.
4. Mariappan R., Kumaran S., Srinivasa Rao T.: Effect of sintering atmosphere on structure and properties of austeno-ferritic stainless steels. Materials Science and Engineering A, 2009, vol. 517, no. 1, pp. 328–333.
5. Rajaguru J., Arunachalam, N.: Coated tool Performance in Dry Turning of Super Duplex Stainless Steel. Procedia Manufacturing, 2017, vol. 10, pp. 601–611.
6. Lailatul P.H., Maleque M.A.: Surface Modification of Duplex Stainless Steel with SiC Preplacement Using TIG Torch Cladding. Procedia Engineering, 2017, vol. 184, pp. 737–742.
7. Ciaś A., Frydrych H., Pieczonka T. Zarys metalurgii proszków. WSiP Warszawa, 1992.
8. Dudek A., Wrońska A., Adamczyk L.: Surface remelting of 316L + 434L sintered steel: microstructure and corrosion resistance. Journal of Solid State Electrochemistry, 2014, vol. 18, no. 11, pp. 2973–2981.
9. Chen X., LI J., Cheng X., Wang H., Huang Z.: Effect of hest treatment on microstructure, mechanical and corrosion properties of austenitic stainless steel 316L using arc additive manufacturing. Materials Science & Engineering A, 2018, vol. 715, pp. 307–314.
10. Falkowska A., Seweryn A., Tomczyk A.: Fatigue life and strength of 316L sintered steel of varying porosity. International Journal of Fatigue, 2018, vol. 111, pp. 161–176.
11. Kazior J., Hebda M.: Właściwości Mechaniczne Infiltrowanych Spiekanych Austenitycznych Stali Nierdzewnych AISI 316L. Inżynieria Materiałowa Materials Engineering, 2006, vol. 27, no. 3, pp. 170–173.
12. Sarjasa H., Kulua P., Juhania K., Viljusb M., Matikainenc V., Vuoristoc P.: Wear resistance of HVOF sprayed coating from mechanically activated thermally synthesized Cr_3C_2–Ni spray powder. Proceedings of the Estonian Academy of Sciences, 2016, vol. 65, pp. 101–106.
13. Krolczyk G., Nieslony P., Legutko S., Hloch S., Samardzic I.: Investigation of selected surface integrity features of duplex stainless steel (DSS) after turning. Metalurgija, 2015, vol. 54, pp. 91–94.

14. Godwin G., Julyes Jaisingh S., Shunmuga Priyan M.: Tribological and Corrosion Behavior Studies on Cr_3C_2–NiCr Powder Coating by HVOF Spray Method – A Review. Journal of Materials Science and Surface Engineering, 2017, vol. 5, no. 2, pp. 537–543.
15. Martín, F., García, C., Blanco, Y.: Influence of residual porosity on the dry and lubricated sliding wear of a powder metallurgy austenitic stainless steel. Wear, 2015, vol. 328–329, pp. 1–7.
16. Bobzin K., Zhao L., Öte M., Königstein T., Steeger M.: Impact wear of an HVOF-sprayed Cr_3C_2–NiCr coating. International Journal of Refractory Metals & Hard Materials, 2018, vol. 70, pp. 191–196.
17. Matikainen V., Bolelli G., Koivuluoto H., Sassatelli P., Lusvarghi L., Vuoristo P.: Sliding wear behaviour of HVOF and HVAF sprayed Cr_3C_2–based coatings. Wear, 2017, vol. 388–389, pp. 57–71.
18. Oke S.R., Ige O.O., Falodun O.E., Okoro. A.M., Mphahlele M.R., Olubambi P.A.: Powder metallurgy of stainless steels and composites: a rewiew of mechanical alloying and Spark plasma sintering. The International Journal of Advanced Manufacturing Technology, 2019, vol. 102, pp. 3271–3290.
19. Vashishtha N., Khatirkar R.K., Sapate S.G.: Tribological behaviour of HVOF sprayed WC–12Co, WC–10Co–4Cr and Cr_3C_2–25NiCr coatings. Tribology International, 2017, vol. 105, pp. 55–68.
20. Gariboldi E., Rovatti L., Lecis N., Mondora L., Mondora G.A.: Tribological and mechanical behaviour of Cr_3C_2–NiCr thermally sprayed coatings after prolonged aging. Surface & Coatings Technology, 2016, vol. 305, pp. 83–92.
21. Yaghtin A.H., Salahinejad E., Khosravifard A., Araghi A., Akhbarizadeh A.: Corrosive wear behavior of chromium carbide coatings deposited by air plasma spraying. Ceramics International, 2015, vol. 41, pp. 7916–7920.
22. Lisiecka B., Dudek A.: Characterization of the Cr_3C_2–NiAl Coatings on Sintered Duplex Stainless Steels. Inżynieria Materiałowa Materials Engineering, 2018, vol. 39, no. 3, pp. 100–104.
23. Dudek A., Lisiecka B.: Surface Treatment Proposals for the Automotive Industry by the Example of 316L Steel. Multidisciplinary Aspects of Production Engineering, 2018, vol. 1, no. 1, pp. 369–376.
24. Klimpel A., Borek A., Klimpel A.S.: Laserowa obróbka warstw wierzchnich części maszyn i urządzeń, Stal-Metale & Nowe Technologie, 2013, no. 9–10, pp. 26–36.
25. Rong Y., Huangi Y., Zhangi G., Mi G., Sha W.: Laser beam welding of 316L T-joint: microstructure, microhardness, distortion and residual stress, International Journal of Advanced Manufacturing Technology, 2017, vol. 90, pp. 2263–2270.
26. Paulraj P., Garg R.: Effect of welding parameters on pitting behaviour of GTAW of DSS and super DSS weldments. Engineering Science and Technology, an International Journal, 2016, vol. 19, no. 2, pp. 1076–1083.
27. Vidyarthy R.S., Dwivedi D.K.: Activating flux tungsten inert gas welding for enhanced weld penetration. Journal of Manufacturing Processes, 2016, vol. 22, pp. 211–228.
28. Lisiecka B., Dudek A.: The Surface Treatment of Sintered Stainless Steel. Terotechnology 2017 – Materials Research Proceedings, 2018, vol. 5, pp. 148–153.
29. Lisiecka B., Dudek A.: Modification of the Surface Layer of Sintered Duplex Stainless Steels Through Alloying Using the GTAW Method. Tribologia, 2018, vol. 278, no. 2, pp. 81–88.
30. Dudek A., Lisiecka B.: The effect of alloying method on the microstructure and properties of the PM stainless steel. 25th Anniversary International Conference on Metallurgy and Materials. TANGER Ltd., Ostrava, 2016, pp. 1045–1050.
31. Dudek A., Lisiecka B., Ulewicz R.: The effect of alloying method on the structure and properties of sintered stainless steel. Archives of Metallurgy and Materials, 2017, vol. 62, pp. 281–287.